Pan, W., Liu, S., Li, S., Cheng, X., Zhang, H., Long, Z., Zhang, T., and Chen, Q. 2019. "A model for calculating single-sided natural ventilation rate in an urban residential apartment," *Building and Environment*, 147: 372-381.

A model for calculating single-sided natural ventilation rate in an urban residential apartment

Wuxuan Pan[a], Sumei Liu[a], Shanshan Li[a], Xionglei Cheng[a], Hao Zhang[a], Zhengwei Long[a,*], Tengfei Zhang[a, b] and Qingyan Chen[c]

* Corresponding author's email address: zwlong@tju.edu.cn

[a]*Tianjin Key Laboratory of Indoor Air Environmental Quality Control, School of Environmental Science and Engineering, Tianjin University, Tianjin, China*
[b]*School of Civil Engineering, Dalian University of Technology, Dalian, China*
[c]*School of Mechanical Engineering, Purdue University, West Lafayette, IN, USA*

ABSTRACT

Natural ventilation is an energy-efficient ventilation method for residential buildings, but it is not easy to determine the natural ventilation rate. This investigation developed a simple model for calculating the ventilation rate for an apartment with single-sided natural ventilation with buoyancy and wind pressure effects, based on a wind-driven model. To validate the model, field measurements were conducted in an apartment in an urban residential building in Tianjin, China. The experiment measured indoor and outdoor air temperature, wind speed and direction, wind pressure coefficient at an opening of the apartment, and ventilation rate through the single opening. The results indicated that the wind pressure coefficients calculated by Eq.12 did not agree well with the measured data. However, most of the measurements show a stronger buoyancy effect than wind pressure effect. Our new model was able to predict the ventilation rate with an average error of 13.1%. When we used six other models found in the literature to predict the ventilation rate, the errors ranged from 12.9% to 46.1%. Thus, not only does our model perform very well in predicting the ventilation rate, but it also shown the Interaction between buoyancy and wind pressure.

Keywords: Buoyancy effect, wind pressure effect, simple model, model comparison, field experiment, validation

Nomenclature

A – opening area	α– an exponent in the wind speed power law
C_d – discharge coefficient	ρ – air density
C_p – pressure coefficient	θ – wind angle clockwise from north
h – opening height	
l – opening width	*Subscript*
P – pressure	ave – average
Q – ventilation rate	cal – calculated
Q_{in} – inflow rate	eff – effective
Q_{out} – outflow rate	i – indoor
T – air temperature	lim – limited
U – wind speed	mea – measured
U_{10} – wind speed at an altitude of 10 m	o – outdoor
z – height from ground	ref – reference position
z_0 – neutral plane height from ground	s – buoyancy pressure driven
	w – wind-driven

1. Introduction

Better ventilation strategies are needed for controlling indoor pollutants[1] in residential buildings in China. Natural ventilation of residential buildings has great potential for reducing energy use[2], achieving thermal comfort[3], and creating a healthy indoor environment[4-9]. Two types of natural ventilation are available: single-sided ventilation and cross ventilation[10]. Although single-sided ventilation is less efficient than cross ventilation, it is more prevalent in residential buildings in urban areas because it is easier to achieve[2, 8, 11]. A survey of window-opening habits of Chinese residents revealed that 86.8% of the residents chose single-sided ventilation in northern China[12]. However, single-sided natural ventilation in urban areas is often affected by the surrounding terrain and surrounding buildings[13] and is highly dependent on the wind environment[14, 15]. It is essential to find a suitable method for determining the ventilation rate provided by single-sided natural ventilation.

Among the existing methods, empirical models can provide rapid estimates of the natural ventilation rate[11,16]. The most widely used and essential empirical model for calculating natural ventilation rate was proposed by Warren[17, 18] on the basis of mixing layer theory. The model calculates wind-driven and buoyancy-driven ventilation rates separately and uses the higher value as the total ventilation rate. To improve Warren's model, Dascalaki et al.[19, 20] multiplied the buoyancy-driven ventilation model by a synthetic factor that is a function of the Grashof number and Reynolds number in place of the discharge coefficient. However, the synthetic factor was obtained by experimental data fitting and did not consider wind direction. From Warren's buoyancy-driven ventilation model, Caciolo et al.[21, 22] converted wind speed into effective temperature difference and developed a new correlation adapted to leeward conditions. Although various correlations have been developed for windward and leeward conditions, they have not reflected the wind angle. Tang et al.[23] found that the above models did not perform well when the temperature difference was less than 1 K, and they developed a model for low wind speed in an urban setting. De Gids and Phaff[24] developed an empirical correlation that considers the impact of both wind and stack pressure on ventilation rate by means of an orifice outflow model. Again, however, the model did not account for wind direction. Larsen and Heiselberg [25] proposed a model that correlated empirical constants with windward, parallel or leeward flow by fitting it with wind tunnel experimental data. However, the model did not cover all the wind directions and did not consider the varied airflow along the height of the opening. We [26] previously developed an empirical model for wind-driven, single-sided ventilation, which accounted for wind velocity profiles and the interaction between window opening and incoming wind. The window type could be sliding, awning, hopper, or casement type. The model quantified the influence of eddy penetration on ventilation rate but did not consider the impact of stack effect on ventilation.

The preceding review shows that none of the models available in the literature is ideal. No model considers wind speed, all directions and air temperature difference at the same time, nor reflects the interaction of wind and buoyancy pressure. It is thus necessary to develop a new model that considers systematically the impact of wind speed, wind direction, and indoor and outdoor air temperature difference on single-sided natural ventilation in an apartment in an urban area. This forms the objective of the investigation reported in this paper.

2. Mathematical model

This investigation sought to expand our previous model[26] to account for stack effect in an apartment with single-sided natural ventilation. The model assumes that the bi-directional flow was non-uniform through the opening and was governed by the wind pressure along the opening. The wind pressure on the surface in the atmospheric boundary layer can be described as[27]

$$P_{wind}(z) = \frac{1}{2}\rho_o C_P U^2(z) \quad (1)$$

The model also assumes that wind speed distribution in an urban setting can be represented by the power law equation [27, 28]

$$U(z) = U_{ref}\left(\frac{z}{z_{ref}}\right)^{\alpha} \quad (2)$$

where α is determined by the terrain category [29], 0.3 in Large city centers; U_{ref} and z_{ref} are wind speed and the height of the reference location, where is at the height of the roof in this investigation, z_{ref}=18m. The model determines the pressure difference that causes flow across the opening from the following equation:

$$\Delta P(z) = \frac{1}{2}\rho_o C_p U^2(z) - P_i \quad (3)$$

This investigation considered the pressure difference caused by the indoor-outdoor air temperature difference by modifying Eq. (3)

$$\Delta P(z) = \frac{1}{2}\rho_o C_p U^2(z) + P_o - P_i - (\rho_o - \rho_i)gz \quad (4)$$

The pressure difference across the opening, $\Delta P(z_0)$, is zero at the neutral plane height ($\Delta P(z_0) = 0$). Then the static pressure difference $(P_i - P_o)(z_0)$ can be expressed as

$$(P_i - P_o)(z_0) = \frac{1}{2}\rho_o C_p U^2(z_0) - (\rho_o - \rho_i)g\rho z_0 \quad (5)$$

and the pressure difference in Eq. (4) along the opening height is

$$\Delta P(z) = \frac{1}{2}\rho_a C_p (U^2(z) - U^2(z_0)) + (\rho_0 - \rho_i)g(z_0 - z) \quad (6)$$

Combined Eq. (1)-(2), Eq. (6) and $Q = \int C_d l \sqrt{\frac{2\Delta P(z)}{\rho}}\, dz$, taking into account the buoyancy effect in our previous model for wind-driven ventilation [26],

$$Q = \frac{C_d l \int_{z_0}^{h} \sqrt{C_p (z^{2\alpha} - {z_0}^{2\alpha})}\, dz}{{z_{ref}}^{\alpha/2}} U_{ref} \quad (7)$$

Then we got the calculation formula of the ventilation rate driven-by buoyancy and wind pressure:

$$Q = C_d l \int_{z_0}^{h} \sqrt{\left| C_p \frac{U_{ref}^2}{z_{ref}^{2\alpha}} \frac{T_i}{T_a} (z^{2\alpha} - {z_0}^{2\alpha}) + \frac{2(T_i - T_o)}{T_a} g(z_0 - z) \right|}\, dz \quad (8)$$

where C_d = 0.6 is a discharge coefficient related to opening characteristics[30, 31] and α is a power law exponent in Eq.(2). The z_0 is neutral plane height [22], which can be obtained by solving the equation

$$Q_{in} = Q_{out} \quad (9)$$

The proposed new model reflects the interaction of wind pressure and stack pressure. Our previous paper [26] explained the physical meaning of the first term in the square root. The physical meaning of the second term is very clearly the pressure difference caused by buoyancy.

3. Field experiment

Due to the difficulty of obtaining the required parameters in Eq. (8) at the same time in previous literatures, to verify the proposed model, this investigation conducted field measurements of the natural ventilation rate under various conditions. This section describes the methods and measured parameters in an apartment located in an urban area in Tianjin, China. The apartment building was 65 m long, 15 m wide and 16 m high, as shown in Fig. 1(a). Our measurements were conducted from March 26, 2017 to November 22, 2017 in a two-bedroom apartment on the third floor of the building (designated with a star in the figure). Fig. 1(b) shows the floor plan of the apartment, and the red box indicates the master bedroom used for measuring single-sided natural ventilation. The master bedroom had an area of 16.98 m^2, including a 3.33 m^2 balcony, and a floor height of 2.6 m. The net volume of the room was 39.83 m^3 with the exclusion of the wardrobe, bed and nightstands. The window had four sliding panes, and the one opened for the experiment had an area of 0.55 m^2 (0.46 m wide and 1.2 m high).

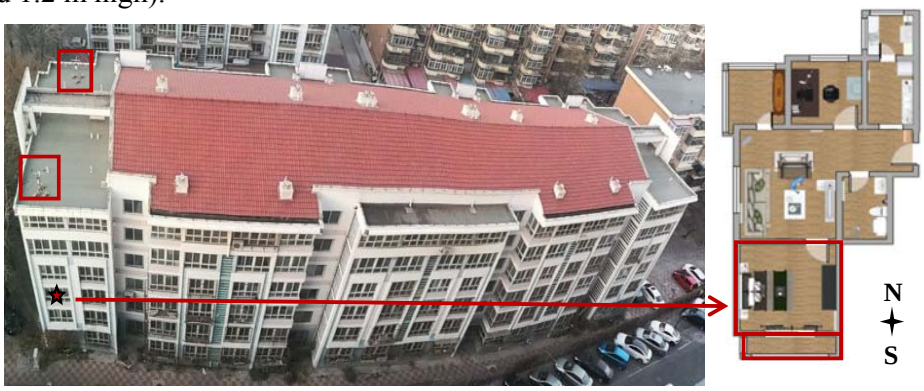

(a) (b)

Fig. 1. *(a) Apartment building in Tianjin, China, with weather stations on the roof as indicated by the two red boxes and (b)floor plan of the two-bedroom apartment*

This investigation measured outdoor wind speed at the reference position (U_{ref}), outdoor air temperature (T_o), indoor air temperature (T_i), wind pressure coefficient (C_p) and ventilation rate (Q). The following subsections will show the detailed experimental methods for measuring these parameters.

3.1 Outdoor weather parameters

Fig.1 (a) also shows two HOBO micro weather stations installed at a height of 2 m above the rooftop of the building for measuring outdoor wind velocity, wind direction, and air temperature. The micro weather stations had a measuring accuracy of ±0.4% for wind velocity when it was greater than 0.5 m/s, ±5° for wind direction, and ±0.2°C for air temperature. The measuring frequency was once per minute. Those values were averaged over the period of the measurements for model validation. Because of the vector nature of wind direction, the average value may not be appropriate, and therefore vector decomposition was adopted. The synthetic wind angle [32] was

$$\theta = tan^{-1}\left(\frac{\sum(U_i \times sin\theta_i)}{\sum(U_i \times cos\theta_i)}\right) \quad (10)$$

where θ is the average wind direction and θ_i is the wind direction of the i-th minute in the experiment data set.

3.2 Indoor temperature

In order to consider the effect of stack pressure on natural ventilation, indoor and outdoor air temperatures were measured with DS18B20 temperature sensors that had an error of ±0.5 K. Because the indoor temperature distribution may not have been uniform, this experiment used eight temperature sensors for measuring the indoor air temperature as shown in Fig. 2, where sensor P1 was placed in the enclosed balcony and other 7 sensors evenly distributed in the three directions of the bedroom. Note that the door between the room and the balcony was open during the experiment.

Fig. 2. *Placement of indoor air temperature sensors*

3.3 Wind pressure coefficient

Eq. (8) contains the wind pressure coefficient, C_p, which accounts for the impact of building shape and wind pressure[33, 34] on natural ventilation. The pressure coefficient can be calculated from the measured static pressure and velocity as:

$$C_p = \frac{P_{wall} - P_{ref}}{{}^1/_2 \rho {U_{ref}}^2(z)} \tag{11}$$

The following empirical equation [35] is used to calculate the wind pressure coefficient from the shape coefficient and wind direction:

$$C_p = 0.6 \times ln\left[1.248 - 0.703\, sin\frac{\beta}{2} - 1.175(sin\,\beta)^2 + 0.131\,(sin\,2\beta G)^3 + 0.769\, cos\frac{\beta}{2} + 0.07G^2(sin\frac{\beta}{2})^2 + 0.717\,(cos\frac{\beta}{2})^2\right] \tag{12}$$

Since the wind pressure coefficient calculated by Eq. (12) may not be accurate, this study also measured the wind pressure coefficient to validate the equation. Measurements of P_{wall} and P_{ref} were conducted by using a low differential pressure transducer with accuracy of 0.4% within the range of ±25 Pa (Setra Model 261C). The measurement frequency for wind pressure was once per minute. The pressure P_{wall} on the surface of the building was determined at the center height of the opening. The wind pressure coefficient was then calculated by Eq. (11) with the use of the measured pressure difference. Fig. 3 shows the locations of the pressure sensors.

Fig. 3. *Schematic of pressure measurement positions near the window and the reference position at the weather station*

3.4 Natural ventilation rate

To measure the ventilation rate in the room with the single-sided opening, one mature and widely used approach is the tracer gas decay method[36-38]. This investigation sealed all the openings at the beginning of the experiment. Next, carbon dioxide as the tracer gas was released into the room, and a fan was used to enhance the mixing in the room until the CO_2 concentration was at least 3500 ppm higher than the outdoor concentration. The fan was then switched off, and a window was opened for about 40 minutes to simulate single-sided ventilation. The window opening was 0.46 m wide and 1.2 m high.

The decay method required complete mixing of the tracer gas in the room. To verify the uniformity of the indoor CO_2 concentration during the experimental period, the concentration was measured at six different locations in the room. The measuring accuracy of the CO_2 sensors is ±50ppm. The results indicated a maximum difference of 240 ppm when the indoor CO_2 concentration reached 3500 ppm. The ventilation rate was determined by using a method from the literature [39].

4. Results

Based on the direct measurement data obtained in section 3, this section describes (1) the experimental results, (2) model validation by experimental results, and (3) the comparison of the proposed model with different previous models.

4.1 Experimental results

This section presents the experimental results obtained from this investigation of single-sided natural ventilation in the apartment in Tianjin from March 26, 2017 to November 22, 2017. The experimental data was intended for validating the proposed model described by Eq. (8).

We conducted 50 sets of measurements under the meteorological conditions with wind direction changed by less than 90° during the experiment. Table 1 shows ten selected sets of data and corresponding standard deviation that are arranged according to increasing indoor-outdoor air temperature difference, from -2.3 K to 13.2 K, and the corresponding wind direction, wind velocity, outdoor air temperature, mean indoor air temperature, and ventilation rate. The table also provides the minimum and maximum ventilation rate. The measurements were conducted with wind angle varying from 14° to 338°, indoor temperature between 288.6 K and 303.2 K, and outdoor temperature ranging from 277.1 K to 303.8 K.

The data provides information about variations in the meteorological parameters and indoor-outdoor air temperature difference. Because of the sheltering effect of the building envelope, the impact of neighboring apartments, indoor heating source and the thermal mass of the apartment, the indoor air temperature varied less than the outdoor air temperature.

Table 1. *Selected sets of measured data*

	T_i-T_o	Direction (°)	U (m/s)	T_o (K)	T_i (K)	ACH (h^{-1})	R^2
	-2.3	251±13	1.98±0.28	303.2±0.1	300.9±0.5	3.14	0.988
	-1.1	245±20	1.95±0.72	301.0±0.5	299.9±0.1	2.78	0.995
	0.4	77±35	0.04±0.12	301.4±0.1	301.8±0.0	1.59	0.996
	1.2	241±19	3.06±1.43	299.2±0.1	300.4±0.3	3.08	0.995
Selected	2.0	244±18	1.93±0.56	287.9±0.2	289.9±1.1	3.28	0.998
data	3.8	242±16	1.59±0.40	293.9±0.2	297.7±0.5	4.09	0.996
	4.6	204±7	1.17±0.31	284.7±0.2	289.3±0.7	4.06	0.998
	7.0	231±19	1.29±0.45	281.6±0.1	288.6±0.9	5.77	0.992
	9.1	90±13	1.19±0.59	282.7±0.0	291.8±1.1	5.00	0.996
	12.1	36±30	0.85±0.48	277.1±0.1	289.2±1.4	6.40	0.988
Min	-2.3	14	0.04	277.1	288.6	1.25	
Max	13.2	338	3.61	303.8	303.2	6.90	

Note that Eq. (8) uses a mean indoor air temperature. The air temperature in the bedroom of the apartment was not uniform. At the maximum indoor-outdoor air temperature difference of 13.2 K, Fig. 4 depicts the indoor air temperature distribution for the positions shown in Fig. 2. The temperature difference along the longitudinal direction was 4.7 K, and along the vertical direction it was 2.6 K.

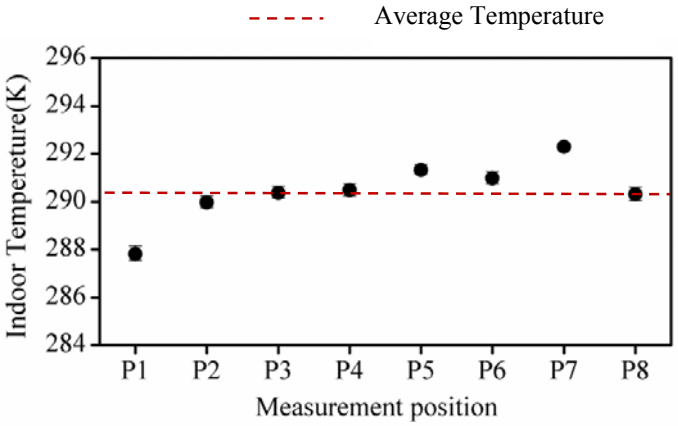

Fig. 4 *Temperature distribution measured in the bedroom at the maximum indoor-outdoor air temperature difference of 13.2 K.*

Measurement of the pressure difference between the reference position and the surface of the window, as shown in Fig. 3, allowed the wind pressure coefficient to be obtained by Eq. (11). Fig. 5 shows the wind pressure coefficients and wind directions from one of the tests, in which the average wind speed was 2.03 m/s. Because of the natural pulsation characteristics of wind, the wind pressure coefficients changed continuously. This study used the average wind pressure coefficient in Eq. (8).

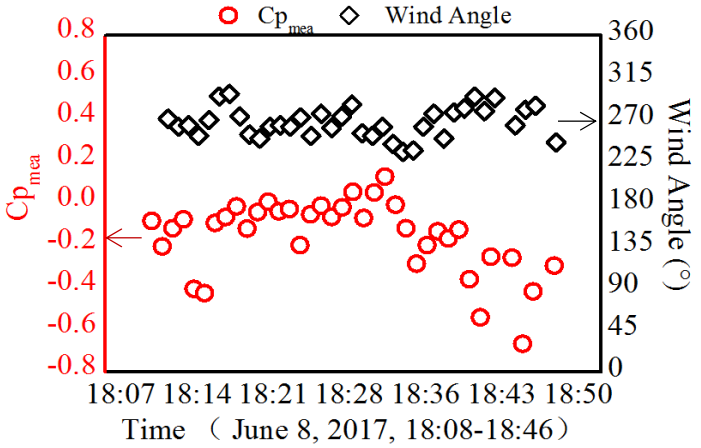

Fig. 5. *Wind pressure coefficient and wind direction in one of the tests*

A key piece of data for validating the proposed model is the ventilation rate, Q, which was obtained experimentally by the tracer-gas method as discussed in Section 3.4. With CO_2 as the tracer gas, Fig. 6 depicts the difference in indoor and outdoor CO_2 concentration in a measurement with an average wind speed of 1.15 m/s and wind direction of 266°. The results were the CO_2 concentration decay over time at six positions in the bedroom. The ventilation rate calculated from the CO_2 concentration decay was averaged at 5.14 ACH with a 0.55 m^2 window opening area for the room. The maximum difference in ventilation rate among those positions was only 4%. Unlike the highly non-uniform air temperature, the CO_2 concentration distribution was fairly uniform. The results demonstrate that the uniformity of the tracer gas decay in the room was acceptable. Therefore, position 6 was used as the sampling point for subsequent ventilation rate measurements.

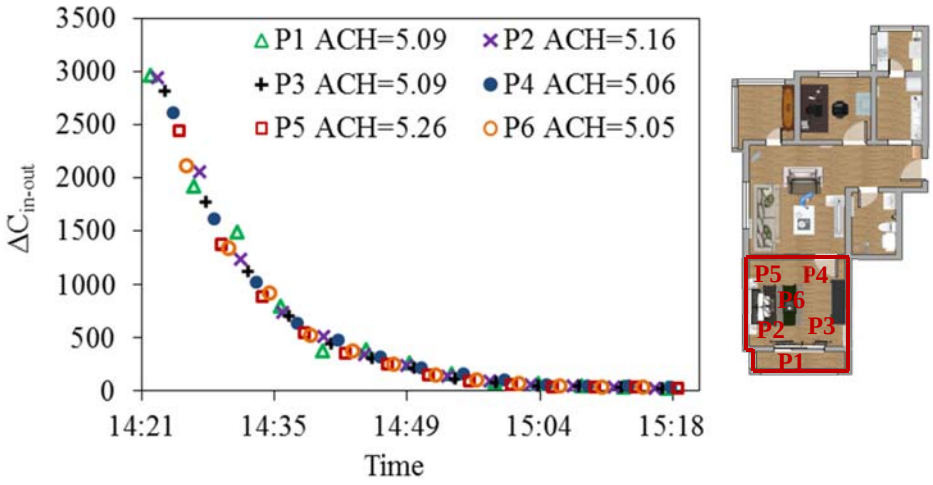

Fig. 6 *CO_2 concentration decay measured at six different positions in the bedroom and the corresponding calculated ventilation rate*

The pressure coefficients on the building surface outside the window were measured as described in Section 3.3. Fig. 7(a) compares the wind pressure coefficients calculated by Eq. (11) with those calculated by Eq. (12) with the use of measured parameters for 10 of the 50 cases. Among the ten cases, six of them exhibited a significant difference. Note that the calculated pressure coefficients were the average surface values for low-rise buildings, which were not the same as the values measured at single points as in this investigation. Also, the

calculated coefficients were for a steady state, whereas the measurements had exhibited significant fluctuations as depicted in Fig. 5. Although the agreement between the calculated and measured wind pressure coefficients was disappointing, it was not a surprise.

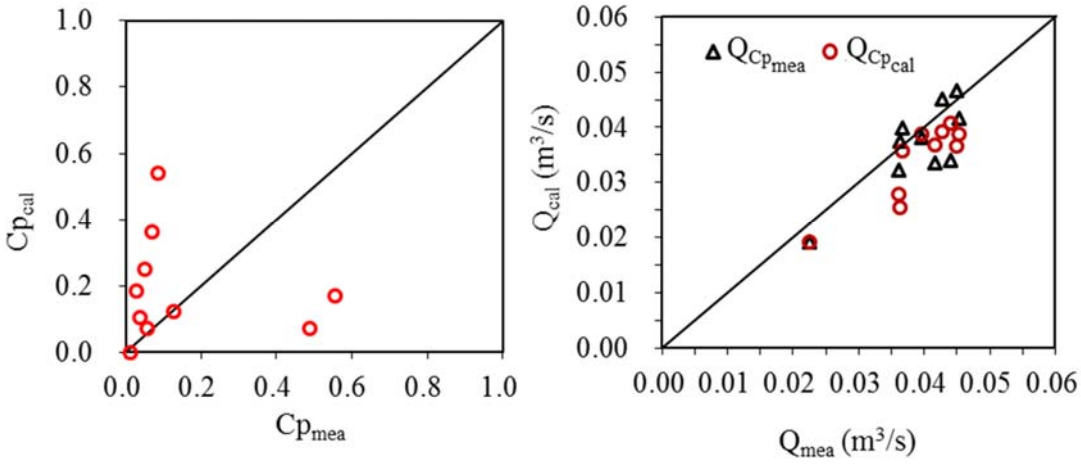

(a) (b)

Fig. 7. Comparison of (a) pressure coefficients and (b) ventilation rates obtained with calculated and measured pressure coefficients

Nevertheless, the ventilation rates determined by the proposed model with the pressure coefficients calculated by Eq. (11) were similar to the rates determined with experimental pressure coefficients calculated by Eq. (12), as shown in Fig. 7(b). In the proposed model, one can see that C_p may not be the dominating factor. The reference wind velocity and neutral plane height were equally important. Taking the case with Cp_{cal} = 0.17 and Cp_{mea} = 0.56 in Fig. 7(a) as an example, the corresponding calculated ventilation rates were 0.041 m^3/s and 0.034 m^3/s, respectively, when all other variables remain unchanged. The difference in the calculated ventilation rates was 17%. Therefore, the proposed model was not very sensitive to the wind pressure coefficient. Fig. 7 shows that the average difference between the measured and calculated ventilation rates was only 13.2%.

4.2 Model validation

This investigation measured 50 sets of single-sided ventilation rates for the apartment with a south-facing opening (window). According to the wind angles, the wind direction at the opening could be classified as windward, parallel, or leeward as shown in Table 2. Fig. 8 displays the average wind angle and speed for the 50 cases. For each type of wind direction, the case numbers increased with increasing $\Delta T = T_i - T_o$.

Table 2 *Relationship between wind direction at the opening and wind angle*

Wind direction	Wind angle
windward	105°-255°
parallel	75°-105°, 255°-285°
leeward	0°-75°, 285°-360°

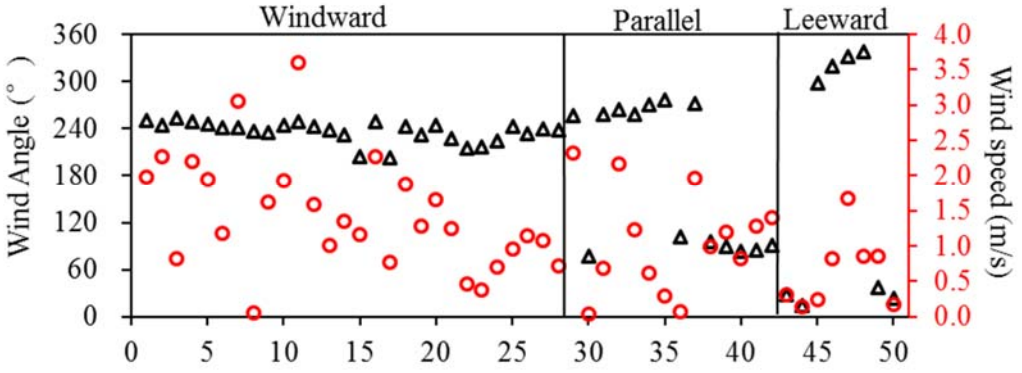

Fig. 8. *Distribution of the average wind angle and speed for the 50 sets of measurements*

Fig. 9 compares the measured ventilation rate with that calculated by the proposed model for different wind directions and speeds under various temperature differences between the indoor and outdoor air. The case numbers in Fig. 9 correspond to those in Fig. 8. As illustrated by Fig. 9, the proposed model in the windward cases had an average error of 12.7%. In the leeward cases, the error was 11.2%, and large errors occurred with a large indoor-outdoor air temperature difference. The proposed model had the worst performance in the parallel cases, with an average error of 15.1%. Because of the complex outdoor airflow near the window, the flow contained numerous eddies of various sizes. The eddy penetration through the opening affected the ventilation rate and may have played a major role in natural ventilation in the parallel cases. In light of the model's simplicity and the fact that it did not account for the fluctuation effect, its performance was not bad.

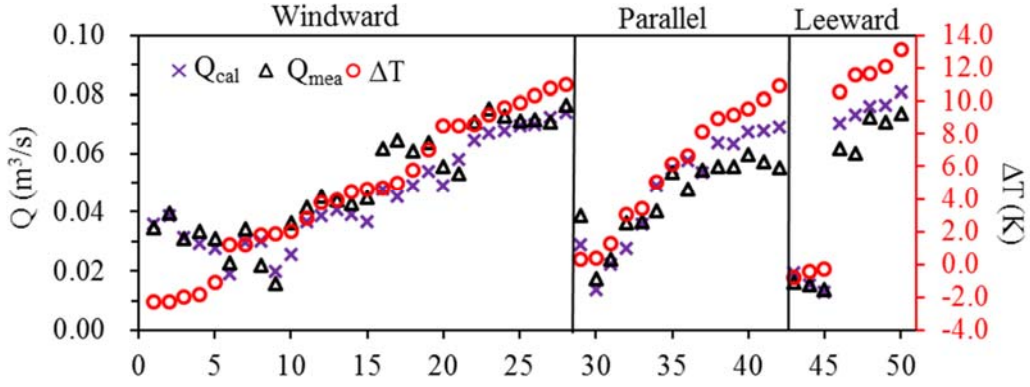

Fig. 9. *Comparison of the calculated and measured ventilation rates for the 50 cases*

Note that the ventilation rate increased approximately with the increase in indoor-outdoor air temperature difference, as illustrated by Fig. 9. When the case numbers were rearranged according to the increase in wind speed for each wind direction, as shown in Fig. 10, the measured and calculated ventilation rates did not show a clear trend of increase with higher wind speed.

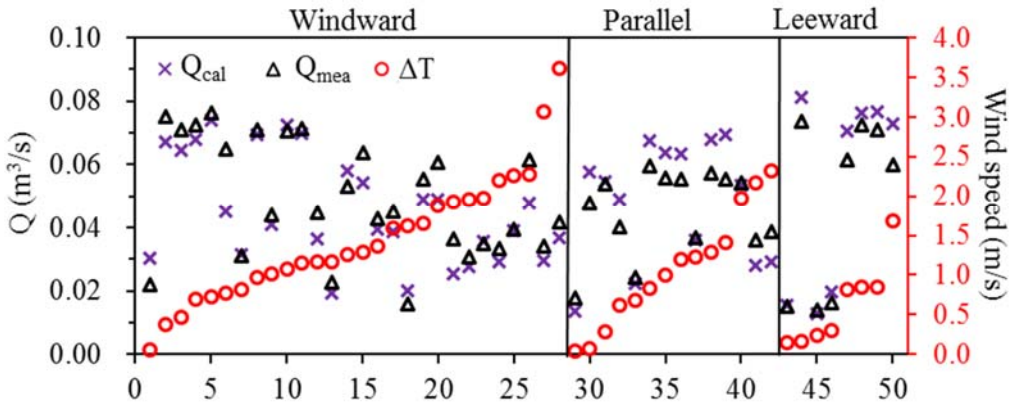

Fig. 10. *Comparison of the calculated and measured ventilation rates with the increase in wind speed*

To further study whether the ventilation in our experiment was dominated by the buoyancy force, the ventilation rates driven by wind pressure and buoyancy force were calculated for each of the 50 cases. In the case of only wind-driven ventilation, Eq. (8) becomes the same as our previous model as:

$$Q_w = \frac{C_d l \sqrt{C_p} \int_{z_0}^{h} \sqrt{z^{2\alpha} - {z_0}^{2\alpha}}\, dz}{z_{ref}^{\alpha}} U_{ref}$$

For only buoyancy-driven ventilation, Eq. (8) is

$$Q_s = C_d l \int_{z_0}^{h} \sqrt{\left|\frac{2(T_i - T_o)}{T_{ave}} g(z_0 - z)\right|}\, dz = \frac{1}{3} C_d A \sqrt{\left|\frac{2g(T_i - T_o)}{T_{ave}} (h - z_0)\right|}\, dz \qquad (13)$$

When the height of the neutral plane is at the middle of the opening ($z_0 = \frac{h}{2}$), Eq. (13) and Warren's buoyancy pressure ventilation model are exactly the same.

Fig. 11 illustrates the ventilation rate determined by wind pressure (Q_w) as calculated by Eq. (7), the rate determined by buoyancy force (Q_s) from Eq. (14), the measured rate (Q_{mea}), and the rate calculated by Eq. (8) for the combined effects of wind pressure and buoyancy force (Q_{cal}). The Q_w was smaller than Q_s even with a small temperature difference between indoor and outdoor air. The Q_s was very close to Q_{mea}, which indicates a strong buoyancy effect. Taking the wind pressure into consideration, Q_{cal} was generally larger than Q_s, but not always. This is because the buoyancy force was not always in the same direction as the wind force, which will be discussed later.

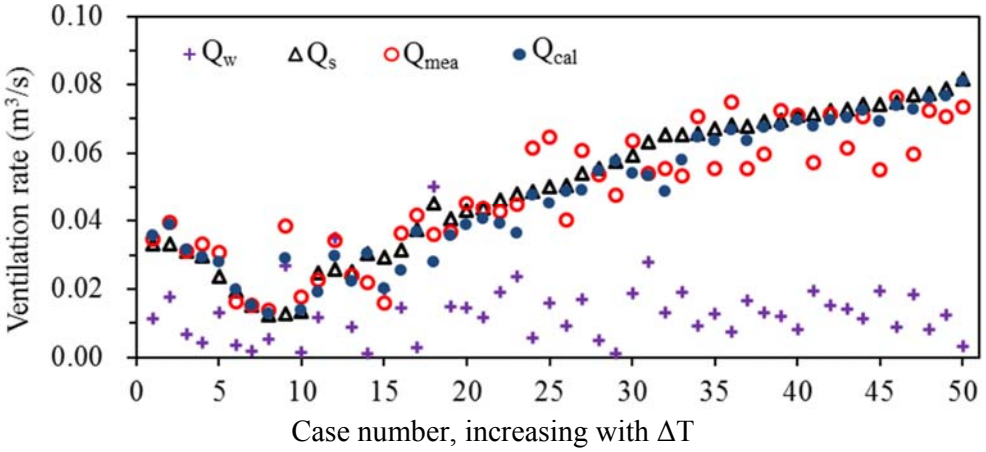

Fig. 11. *Comparisons of the ventilation rates calculated by different models with the measured data*

Because of the attenuation of wind speed by the urban ground roughness and surrounding buildings, the wind speed in the urban area rapidly decreased. As shown in Fig. 8, the wind speed at the reference position was generally less than 2 m/s. As the opening was not very large, the wind-driven ventilation rate was quite low. Thus, the single-sided natural ventilation in our study was dominated by the temperature difference between the indoor and outdoor air.

4.3 Comparisons with previous models

Although the model proposed here performed fairly well according to the comparison of predicted and measured ventilation rate, this investigation took the additional step of comparing the performance of our model with other popular models found in the literature. The comparison was made for various wind speeds and indoor-outdoor air temperature differences.

Our previous model[26] was developed for wind-driven natural ventilation under isothermal conditions and is actually our base model without considering thermal buoyancy. The ventilation rate is determined by Eq. (13). Fig. 12 compares the ventilation rates calculated by Eq. (13) and the new model with our experimental data. In the selected cases, the indoor-outdoor air temperature difference was less than 1.8 K. In a completely isothermal case, our present and previous models would be exactly the same. The differences shown in the figure indicate that even a small temperature difference between indoor and outdoor air could cause some degree of difference in the two models' predictions of ventilation rate. Our previous model predicted lower ventilation rate when buoyancy was not taken into account, which is understandable. Thus, the effect of thermal buoyancy should not be neglected.

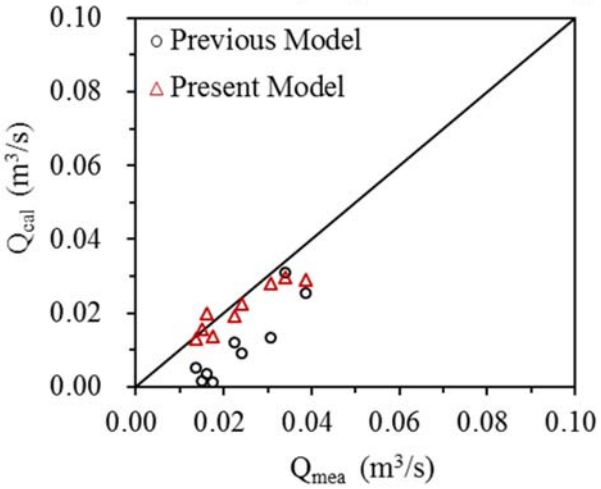

Fig. 12. *Comparison of the ventilation rates calculated by our previous model[26] and present model with the measured data*

We compared the performance of our model with that of six other models from the literature. Warren's model calculates the wind-driven and buoyancy-driven ventilation rates, respectively, as

$$Q_w = 0.025 A_{eff} U \tag{14}$$

$$Q_s = \frac{1}{3} A_{eff} C_d \sqrt{\frac{gh\Delta T}{T_{ave}}} \tag{15}$$

The larger of Q_w and Q_s was taken as the total ventilation rate. In fact, when either the buoyancy pressure or wind pressure played a dominant role, the model ignored the influence of the other. Fig. 13(a) compares the performance of our model with Warren's model. Since

the cases were dominated by the buoyancy effect, the impact of the wind pressure was not very evident. Our model had a 13.1% average error while Warren's model had an average error of 14.7%. Our model performed slightly better than Warren's model because the impact of pressure was included in our model.

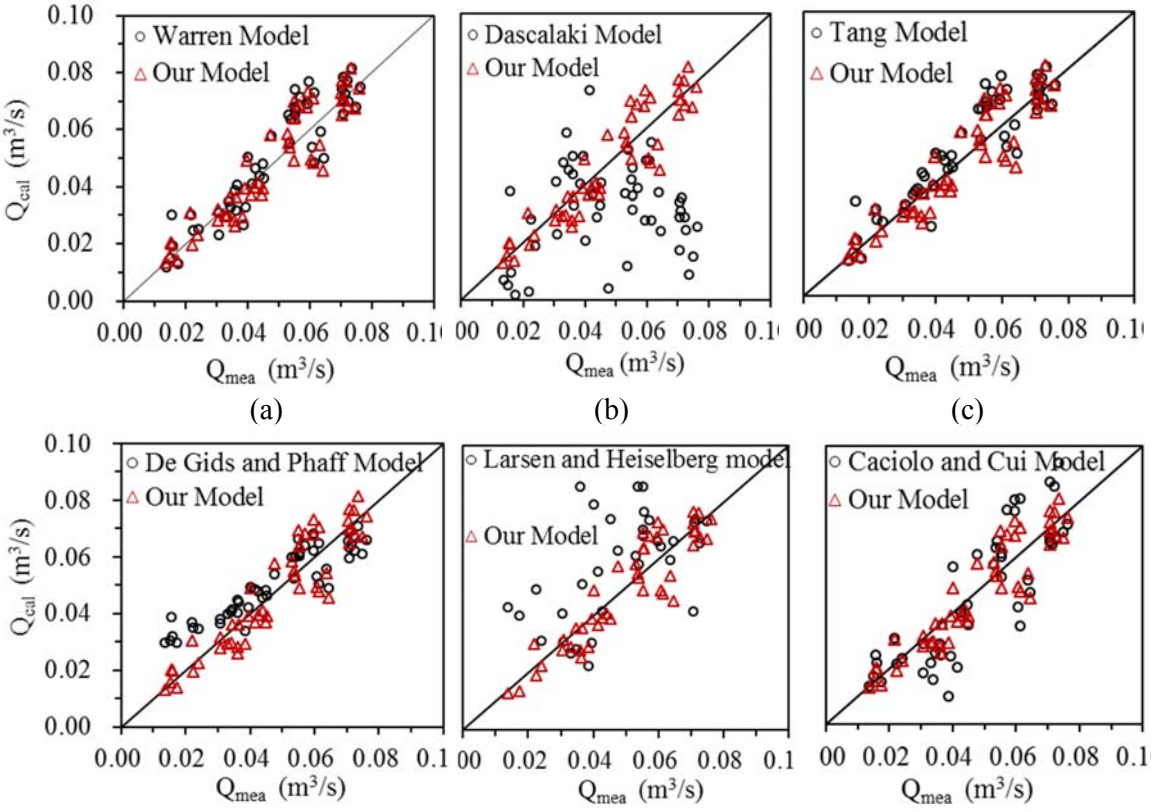

Fig. 13. *Comparison of the performance of our model with the models from Warren [17], Dascalaki et al.[19], Tang et al.[23], De Gids and Phaff [24], Larsen and Heiselberg [25] and Caciolo and Cui [21] with the use of our measured data as a reference.*

Dascalaki et al.[19] used a correction parameter CF that is a function of the Grashof and Reynolds numbers to replace the discharge coefficient in predicting the total ventilation rate by

$$Q = CF \cdot \frac{1}{3} A \sqrt{\frac{gh(T_i - T_o)}{T_i}} \text{ with } CF = 0.08(Gr/Re_D^2)^{-0.38} \quad (16)$$

where the constant and exponent in the CF calculation were obtained by fitting with their experimental data. Fig. 13(b) shows that their model did not perform as well as our model. The average error of their model was 46.1%, which was close to that found in other studies [23]. The key is to obtain the correct CF. The empirical fitting parameters used by Dascalaki et al. would depend very much on the similarity of the experimental data and the case to be predicted.

Experimental results obtained in primary schools in Beijing by Tang et al. [23] indicated that some previous models had large errors when the local wind speed was less than 1 m/s. By fitting with their data, Tang et al. obtained an empirical correlation coefficient for local wind speed less than 1 m/s ($U_L < 1\ m/s$) that was based on Warren's model, as follows:

$$Q = C_d \cdot \frac{1}{3} A \sqrt{\frac{gh|T_i - T_o|}{T_i} + \frac{C}{|T_i - T_o|}} \quad (17)$$

Fig. 13(c) compares Tang's (2016) model and our model for $U_L < 1\,m/s$ in our experiments. Their model performed very well with an average error of 12.9%, compared with our model with 13.1% error. Since their experiment was performed under similar weather conditions to ours, the empirical correlation coefficient would be very suitable for our cases. Therefore, such good performance should not be surprising. Whether or not their empirical correlation coefficient would work for other weather conditions is unknown. Nevertheless, our model's performance is no poorer than that of their model.

De Gids and Phaff [24] developed a correlation to calculate ventilation rate from a combination of wind, buoyancy, and fluctuation by

$$Q = \frac{1}{2} A \sqrt{\left(0.001 {U_{10}}^2 + 0.0035 h \Delta T + 0.01\right)} \quad (18)$$

Fig. 13(d) compares the performance of De Gids and Phaff's model with that of our model. The constants in the equation were obtained from their experimental data without considering wind angles or the sign of ΔT. Their model overestimated ventilation rates in most cases and had an average error of 24.2%. Obviously, the wind angle and the sign of ΔT are important factors in the ventilation rate.

Larsen and Heiselberg [25] developed the following model by using wind tunnel experimental data and taking into account limited wind directions (windward, parallel and leeward):

$$\mathrm{Q} = A \sqrt{C_1 f(\beta_v)^2 \left|C_p\right| U^2 + C_2 h \Delta T + \frac{\Delta C_{p,opening}(\beta_v) \Delta T}{U^2}} \quad (19)$$

where C_1 and C_2 are empirical parameters related to wind directions, and $f(\beta_v)$ and $\Delta C_{p,opening}$ are functions related to incidence angle β_v. Fig. 13(e) illustrates the performance of the model for our cases. Their model had an average error of 24.1%. In a few cases, the errors were very significant. A possible reason is that their data did not fully cover our cases.

Caciolo and Cui [21] developed two models to predict windward and leeward ventilation, respectively, through CFD simulations. For windward ventilation,

$$Q = Q_s + Q_w = \frac{1}{3} A C_d \sqrt{\frac{gh\Delta T_{eff}}{T_{ave}}} + 0.00357 A (U - U_{lim}) \quad (20)$$

where effective air temperature difference $\Delta T_{eff} = \Delta T(1.234 - 0.490U + 0.048U^2)$ and $U_{lim} = 1.23 m/s$. For leeward ventilation,

$$Q = Q_{s,eff} = \frac{1}{3} A C_d \sqrt{\frac{gh\Delta T_{eff}}{T_{ave}}};\ \Delta T_{eff} = \Delta T(1.355 - 0.179 U_{lim}) \quad (21)$$

where $Q_{s,eff}$ is the effective ventilation rate driven by the buoyancy force. Although the models were designed for windward and leeward conditions, respectively, Fig. 13(f) shows that their models had an average error of 22.3% in predicting our cases. The approximations used in CFD, wind angles, etc., could have contributed to the error.

The above comparison demonstrates that our model is one of the most successful in predicting the natural ventilation rate through a single opening. The prediction had an average error of 13.1%, which is acceptable for design practice.

5. Discussion

The models found in our literature review did not emphasize the significance of the sign in the indoor-outdoor temperature difference, $\Delta T = T_i - T_o$. Because of the thermal inertia of the building used in our experiment, it was possible for the indoor temperature to be lower

than the outdoor temperature in the transitional season, as found in several cases shown in Fig. 9. The proposed model considered the sign of ΔT, which could be important for the interaction between the wind force and the buoyancy force. If the wind pressure in the outdoor space was positive, when $T_i > T_o$, the air would have flowed in through the lower part of the window opening, and the buoyancy force would have enhanced ventilation. When $T_i < T_o$, the ventilation would have been hindered by the buoyancy force. Our model could correctly deal with the sign of ΔT, whereas the other models could not.

Most of the investigations in the literature considered indoor air temperature to be higher than that outdoors [17-24]. As shown in Fig. 14, we found these models from De Gids and Phaff, Larsen and Heiselberg, and Caciolo and Cui performed better with $T_i > T_o$ than $T_i < T_o$ for the 50 cases displayed in Fig. (8). Since there were not many cases with $T_i < T_o$, the models should not produce overly large errors when the sign of ΔT is not taken into account.

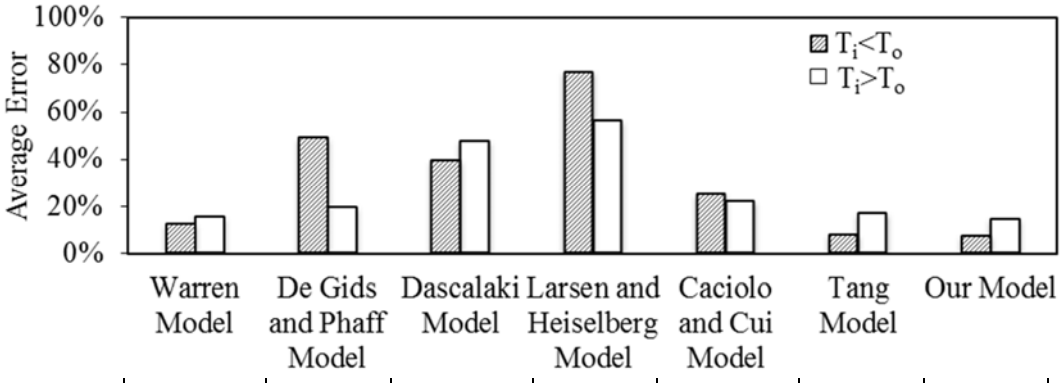

	Warren Model	De Gids and Phaff Model	Dascalaki Model	Larsen and Heiselberg Model	Caciolo and Cui Model	Tang Model	Our Model
$T_i<T_o$	12.2%	47.8%	39.4%	76.8%	24.8%	7.6%	7.2%
$T_o<T_i$	15.2%	19.5%	47.4%	56.0%	21.9%	16.7%	14.3%

Fig. 14. *The impact of $\Delta T = T_i - T_o$ on the errors in the ventilation rate calculated by different models.*

In addition, near the windows it is street canyon, where the wind environment is strongly influenced by the configuration of the street canyon [40, 41]. Then the power law wind profile used to predict the wind speed at the window would bring unpredictable errors, and varied with the environment around the residence. The wind pressure coefficient in the proposed model was the surface average result for an isolated building obtained through empirical correlation. It is not certain what the errors would be for an apartment with many surrounding buildings. The wind pressure coefficient is normally linked to the undisturbed airstream from the upwind direction. This is difficult to determine in an urban environment with complex city topography and skyline. All of these factors would make the calculation of ventilation rate through a single opening very challenging.

6. Conclusions

This investigation developed a new model with considerable physical significance for single-sided natural ventilation driven by wind pressure and buoyancy force, on the basis of our previous study. The model was validated by measured data obtained in an apartment in an urban area. The study led to the following conclusions:

- When the 50 sets of ventilation data obtained in the apartment are used for comparison, our model is able to predict the natural ventilation rate with an average error of 13.1%. The data include a single opening with airflow in windward, parallel, and leeward directions and an indoor-outdoor air temperature difference ranging from

-2.3 K to 13.2 K. The data show that the buoyancy force in our measured data was higher than the wind pressure force because of the high urban building density.

- This investigation also assessed the performance of six other models found in our literature review. Some of the models were purely empirical. Those models calculated the natural ventilation rates through the opening with an average error ranging from 12.9% to 46.1%. Thus, our model performed well in comparison with the other models.
- Our model takes into account the impact of both positive and negative buoyancy forces on natural ventilation through a single opening with outside air pressure, whereas the other models may not do so. However, the wind profile in an urban environment may not be described by a power-law equation, and the pressure distribution on the building envelope was different from that for a single building in an open area. Thus, it was difficult to calculate the wind pressure coefficient of the apartment with reasonable accuracy.

Acknowledgement

This study was supported by the National Key R&D Program of the Ministry of Science and Technology, China, on "Green Buildings and Building Industrialization" through Grant No. 2016YFC0700500 and by the Key Project of the Applied Basic and Frontier Technology Research Program, Tianjin Commission of Science and Technology, China, through Grant No. 15JCZDJC40900.

References

[1]. W. Ye, X. Zhang, J. Gao, G. Cao, X. Zhou, X. Su. Indoor air pollutants, ventilation rate determinants and potential control strategies in Chinese dwellings: A literature review. Science of The Total Environment, 586 (2017) 696-729.

[2]. C. Allocca, Q. Chen, L.R. Glicksman, Design analysis of single-sided natural ventilation. Energy and Buildings, 35 (2003) 785-795.

[3]. X. Su, X. Zhang, J. Gao, Evaluation method of natural ventilation system based on thermal comfort in China. Energy and Buildings, 41 (2009) 67-70.

[4]. Y. Li, P. Heiselberg. Analysis methods for natural and hybrid ventilation - A critical literature review and recent developments. International Journal of Ventilation, 1 (2003) 3-20.

[5]. H. Qian, Y. Li, W.H. Seto, P. Ching, W.H. Ching, H.Q. Sun, Natural ventilation for reducing airborne infection in hospitals. Building and Environment, 45 (2010) 559-565.

[6]. Z. Zhai, M.H. Johnson, M.E. Mankibi, Review of natural ventilation models. Energy Procedia, 78 (2015) 2700-2705.

[7]. M.Z.I. Bangalee, S.Y. Lin, J.J. Miau, Wind driven natural ventilation through multiple windows of a building: A computational approach. Energy and Buildings, 45 (2012) 317-325.

[8]. Z.T. Ai, C.M. Mak, D.J. Cui, On-site measurements of ventilation performance and indoor air quality in naturally ventilated high-rise residential buildings in Hong Kong. Indoor and Built Environment, 24 (2015) 214-224.

[9]. J. Wang, S. Wang, T. Zhang, F. Battaglia, Assessment of single-sided natural ventilation driven by buoyancy forces through variable window configurations. Energy and Buildings, 139 (2017) 762-779.
[10]. Z. Feng, X. Zhou, S. Xu, J. Ding, S. Cao. Impacts of humidification process on indoor thermal comfort and air quality using portable ultrasonic humidifier. Building and Environment, 2018, 133:62-72.
[11]. S. Marzban, L. Ding, F. Fiorito, An evolutionary approach to single-sided ventilated façade design. Procedia Engineering, 180 (2017) 582-590.
[12]. K. Huang, G. Feng, H. Li, S. Yu, Opening window issue of residential buildings in winter in north China: A case study in Shenyang. Energy and Buildings, 84(2014) 567-574.
[13]. T. V. Hooff, B. Blocken, Coupled urban wind flow and indoor natural ventilation modelling on a high-resolution grid: A case study for the Amsterdam ArenA stadium. Environmental Modelling and Software, 25 (2010) 51-65.
[14]. H. W. Tieleman, R.E. Akins, P.R. Sparks, A comparison of wind-tunnel and full-scale wind pressure measurements on low-rise structures. Journal of Wind Engineering and Industrial Aerodynamics, 8 (1981) 3-19.
[15]. Q. Ke, H. Tan, W. Zhu, M. Li, Study on influences of wind characteristics on natural ventilation effect in welding plant. Building Energy and Environment, 26(2017) 97-99.
[16]. Z. T. Ai, C.M. Mak, Determination of single-sided ventilation rates in multistory buildings: Evaluation of methods. Energy and Buildings, 69 (2014) 292-300.
[17]. P. Warren, Ventilation through openings on one wall only, in: Proceedings of International Centre for Heat and Mass Transfer Seminar “Energy Conservation in Heating, Cooling, and Ventilating Buildings”, Washington, 1977.
[18]. P. R. Warren, L.M. Parkins, Window-opening behavior in office buildings. Building Services Engineering Research and Technology, 5 (1984) 89-101.
[19]. E. Dascalaki, M. Santamouris, A. Argiriou, C. Helmis, D.N. Asimakopoulos, K. Papadopoulos, A. Soilemes, On the combination of air velocity and flow measurements in single sided natural ventilation configurations. Energy & Buildings, 24(1996) 155-165.
[20]. E. Dascalaki, M. Santamouris, D.N. Asimakopoulos, On the use of deterministic and intelligent techniques to predict the air velocity distribution on external openings in single-sided natural ventilation configurations. Solar Energy, 66(1999) 223-243.
[21]. M. Caciolo, S. Cui, P. Stabat, D. Marchio, Development of a new correlation for single-sided natural ventilation adapted to leeward conditions. Energy and Buildings, 60 (2013) 372–382.
[22]. M. Caciolo, P. Stabat, D. Marchio, Full scale experimental study of single-sided ventilation: Analysis of stack and wind effects. Energy and Buildings, 43 (2011) 1765–1773.
[23]. Y. Tang, X. Li, W. Zhu, P.L. Cheng, Predicting single-sided airflow rates based on primary school experimental study. Building and Environment, 98 (2016) 71-79.
[24]. W. De Gids, H. Phaff, Ventilation rates and energy consumption due to open windows: A brief overview of research in the Netherlands, Air Infiltration Review, 4 (1982) 4–5.
[25]. T. Larsen, P. Heiselberg, Single-sided natural ventilation driven by wind pressure and temperature difference. Energy and Buildings, 2008, 1031-1040.
[26]. H. Wang, Q. Chen, A new empirical model for predicting single-sided wind-driven natural ventilation in buildings. Energy and Buildings, 2012, 54: 386-394.
[27]. S. Liu, W. Pan, H. Zhang, X. Cheng, Z. Long, Q. Chen, CFD simulations of wind distribution in an urban community with a full-scale geometrical model. Building and Environment, 2017, 117:11-23.

579 [28]. J. Counihan, Adiabatic atmospheric boundary layer: a review and analysis of data from
580 the period 1880–1972, Atmospheric Environment 10 (9) (1975)871–905.
581 [29]. M. Sherman, M. Modera, Comparison of measured and predicted infiltration using the
582 LBL infiltration model, in Proceedings Measured Air Leakage of Buildings,
583 Philadelphia. 1986, pp. 325-347.
584 [30]. Muthusamy V. Swami and Subrato Chandra. Procedures for Calculating Natural
585 Ventilation Airflow Rates in Buildings. Tech. Rep., 1987.
586 [31]. Y. Li, Buoyancy-driven natural ventilation in a thermally stratified one-zone building.
587 Building and Environment, 2000, 35(3):207-214.
588 [32]. S. Han, Y. Liu, W. Yang, G. Jiang, C. Sheng, An optimized vector average method for
589 calculation of average wind direction. Power System Technology, 2015,36(5):68-72.
590 [33]. Y. Guan, A. Li, Y. Zhang, C. Jiang, Q. Wang, Experimental and numerical investigation
591 on the distribution characteristics of wind pressure coefficient of airflow around
592 enclosed and open-window buildings. Building Simulation, 2016, 9(5):551-568.
593 [34]. ASHRAE, Chapter 24 Airflow around buildings, 2009.
594 [35]. M. V. Swami, S. Chandra, Correlations for pressure distribution of buildings and
595 calculation of natural-ventilation airflow, ASHRAE Transactions, 1988, 94: 244–266.
596 [36]. M. H. Sherman, Tracer-gas techniques for measuring ventilation in a single zone.
597 Building and Environment. 1990, 25: 365–374.
598 [37]. S. Cui, M. Cohen, P. Stabat, D. Marchio, CO2 tracer gas concentration decay method
599 for measuring air change rate. Building and Environment, 2015, 84: 162-169.
600 [38]. Y. Choinière, Wind induced natural ventilation of low-rise buildings for livestock
601 housing by the pressure difference method and concentration decay method
602 [microform]. 1991.
603 [39]. X. Dai, J. Liu, Y. Yin, X. Song, S. Jia, Modeling and controlling indoor formaldehyde
604 concentrations in apartments: On-site investigation in all climate zones of China.
605 Building and Environment, 2018, 127:98-106.
606 [40]. J. Hang, Y. Li, M. Sandberg. Experimental and numerical studies of flows through and
607 within high-rise building arrays and their link to ventilation strategy. Journal of Wind
608 Engineering & Industrial Aerodynamics, 2011, 99:1036-1055.
609 [41]. J. Hang, M. Sandberg, Y. Li. Effect of urban morphology on wind condition in
610 idealized city models. Atmospheric Environment, 2009, 43:869-878.